DOI 10.1007/s10958-014-2153-z
Journal of Mathematical Sciences, Vol. 203, No. 4, December, 2014

TRANSONIC GAS FLOW WITH NONPLANAR SHOCK WAVES

M. Yu. Kazakova

Novosibirsk State University
2, ul. Pirogova, Novosibirsk 630090, Russia
m.u.kazakova@gmail.com

UDC 533

We study invariant solutions to the Karman–Guderley equation governing a three-dimensional gas flow with shock waves on nonplanar surfaces. We investigate the global behavior of integral curves and use the obtained result for constructing a solution. Bibliography: 7 *titles. Illustrations*: 5 *figures.*

One of the simplest transonic gas flow models includes the nonlinear Karman–Guderley equation for perturbations of a uniform flow moving with the sound speed [1, 2]. In the case of planar gas flows, exact solutions to the Karman–Guderley equation were considered in [1]–[3], where the equation was linearized by the hodograph transformation. In the case of general spatial gas flows, it is known that there exist solutions described by algebraic functions [4]. A systematic classification and analysis of invariant-group solutions to the Karman–Guderley equation can be found in [5].

In this paper, we study invariant solutions to the Karman–Guderley equation governing three-dimensional gas flows with shock waves on nonplane surfaces. Such solutions exist for two submodels that are reduced to ordinary differential equations of the second order. We make a qualitative analysis of integral curves on the phase plane for each of the equations. In both cases, we show that a unique integral curve corresponding to the solution with shock wave is the separatrix of a saddle singular point. To construct the solution, we study the global behavior of separatrices. We find parameters for which there are conjugate points on the separatrix that satisfy the Rankine–Hugoniot conditions on a shock wave. The study of periods of the obtained solutions shows that several nested shock waves can occur on helical surfaces.

1 The Karman–Guderley Equation

We consider the nonlinear Karman–Guderley equation [1, 2, 6]:

$$-\varphi_x\varphi_{xx} + \varphi_{yy} + \varphi_{zz} = 0. \tag{1}$$

Translated from *Vestnik Novosibirskogo Gosudarstvennogo Universiteta: Seriya Matematika, Mekhanika, Informatika* **13**, No. 1, 2013, pp. 57–67.

We briefly discuss the derivation of this equation. Following [1], for a small parameter we take the deviation of the gas velocity from the sound speed. As is shown in [1, P. 23–29] on the basis of the Rankine–Hugoniot formulas for the compression wave, the entropy change on the shock wave has the third order of smallness. Therefore, we ignore the entropy changes in the first approximation under the assumption that the flow is isentropic. Moreover, the entropy increase condition on the compression jump is replaced by the condition $[\varphi_x] < 0$. It was also shown that the flow is irrotational.

Such flows are governed by the following equation for the velocity potential:

$$(u^2 - c^2)\Phi_{xx} + (v^2 - c^2)\Phi_{yy} + (w^2 - c^2)\Phi_{zz} + 2uv\Phi_{xy} + 2uw\Phi_{xz} + 2vw\Phi_{yz} = 0 \tag{2}$$

and the Bernoulli integral

$$\frac{1}{2}(u^2 + v^2 + w^2) + \frac{c^2}{\gamma - 1} = \frac{1}{2}c_*^2 + \frac{c_*^2}{\gamma - 1}, \tag{3}$$

where $u = \Phi_x$, $v = \Phi_y$, and $w = \Phi_z$ are components of the velocity vector, c is the sound speed, and c_* is the critical sound speed. For the sake of simplicity we consider a polytropic gas and denote by γ the adiabatic exponent.

We study small perturbations of the flow moving with the sound speed along the Ox-axis: $u = c_*$, $v = 0$, $w = 0$, $c = c_*$. The model is constructed in accordance with the formulas [6]:

$$\begin{aligned} &x = \varepsilon^{1+k}x', \quad y = \varepsilon^k y', \quad z = \varepsilon^k z', \\ &\Phi = c_*(x + \varepsilon^{3+k}\varphi'(x', y', z')), \quad c = c_*(1 + \varepsilon^2 c'), \end{aligned} \tag{4}$$

where k is an arbitrary real parameter. By (4), the components of $\mathbf{u} = \nabla\Phi$ are expressed by

$$\begin{aligned} u &= c_*(1 + \varepsilon^2\varphi'_{x'}) = c_*(1 + \varepsilon^2 u'(x', y', z')), \\ v &= c_*\varepsilon^3\varphi'_{y'} = c_*\varepsilon^3 v'(x', y', z'), \\ w &= c_*\varepsilon^3\varphi'_{z'} = c_*\varepsilon^3 w'(x', y', z'). \end{aligned} \tag{5}$$

We make the standard assumption that the functions u', v', w', c', as well as their derivatives for fixed x', y', z', have finite limits as $\varepsilon \to 0$. Substituting (4) and (5) into (2) and (3) and making certain transformation with fixing only terms of lower order with respect to ε (cf. details in [6]), we obtain the equation

$$-(\gamma + 1)\varphi'_{x'}\varphi'_{x'x'} + \varphi'_{y'y'} + \varphi'_{z'z'} = 0.$$

Equation (1) is obtained by introducing the new function $\varphi = (\gamma+1)\varphi'$ and omitting the primes at the variables x', y', z'.

The parameter k can be taken arbitrary because Equations (2), (3) admit the stretch group $\mathbf{x} \to \alpha\mathbf{x}$, $\Phi \to \alpha\Phi$. However, to solve problems in practice, one sets $k = -1$ or $k = 0$. In the case $k = -1$, for modeling (5) the coordinate x "along" the flow remains unchanged. At the same time, $y' = \varepsilon y$, $z' = \varepsilon z$, i.e., the coordinate grid contracts in the transversal direction to the flow approaching the Ox-axis. This allows us to describe correctly slight changes of the flow in the "transversal" direction. The case $k = -1$ is usually used for studying flows around thin bodies of finite length (the body size along the flow remains unchanged).

In the case $k = 0$, only the coordinate x changes in (5). This means that the geometric parameters of the flow in the "transversal" direction remain unchanged. At the same time,

$x = \varepsilon x'$, i.e., in the coordinates (x', y, z), the flow dilates along the Ox-axis. This allows us to describe in detail singularities of the flow near the central part. Such an approach is used for describing transonic gas flows in nozzles and jets (the transverse size of flow is fixed).

For physical interpretation of the flow characteristic are the following objects: the surface of strong discontinuity (of the shock wave), the sound and characteristic surfaces. We write the Rankine–Hugoniot conditions on the shock wave, given by the equation $h(x, y, z) = 0$ [1]:

$$\Big[-\frac{1}{2}\varphi_x^2 h_x + \varphi_y h_y + \varphi_z h_z\Big] = 0, \quad [\varphi] = 0, \quad [\varphi_x] < 0. \tag{6}$$

Hereinafter, we use the square brackets to denote the jump of a function through the surface of strong discontinuity: $[f] = f_2 - f_1$, the state before the wave is marked by the subscript 1. In the submodels under consideration the solution is invariant from both sides of the shock wave. Consequently, the shock wave $\lambda = \text{const}$ is invariant under the same transformation [7].

The sound surface is defined by $\varphi_x = 0$, subsonic flows are characterized by $\varphi_x < 0$ and supersonic flows correspond to $\varphi_x > 0$. Finally, characteristics of the form $h(x, y, z) = \text{const}$ of Equation (1) are determined on the solution $\varphi = \varphi(x, y, z)$ to the equation $-\varphi_x h_x^2 + h_y^2 + h_z^2 = 0$. In the cylindrical coordinates (x, r, θ), the equation for characteristic surfaces has the form

$$-\varphi_x h_x^2 + h_r^2 + \frac{h_\theta^2}{r^2} = 0. \tag{7}$$

Now ,we proceed with invariant submodels of Equation (1).

2 Invariant Submodel of Rank 1

For classifications of invariant submodels of Equation (1) we refer to [5]. We consider submodels of rank 1 (i.e., submodels reducible to an ordinary differential equation), where the invariant variable λ linearly depends on the polar angle θ in the cylindrical coordinates (x, r, θ). These submodels are described in the table below. The submodel numbers in the first column correspond to the classification in [5]. According to the second column, the invariant variable linearly depends on the polar angle. This means that for the continuity of the solution in the entire space the function $B(\lambda)$ must be $2\pi\alpha$-periodic.

TABLE. Invariant submodels of Equation (1) of rank 1

	Representation of solutions	Equations of submodel
2.1.	$\varphi = x^3 r^{-2} B(\lambda)$, $\lambda = \alpha\theta + \beta \ln r - \ln \lvert x \rvert$	$(\alpha^2 + \beta^2 - 3B + B')B'' - 5(B')^2 + (-4\beta + 21B)B' + 4B - 18B^2 = 0$
2.3.	$\varphi = r^{-2} B(\lambda)$, $\lambda = x - \alpha\theta - \ln r$	$(1 + \alpha^2 - B')B'' + 4B' + 4B = 0.$
2.4.	$\varphi = r^{-2} B(\lambda)$, $\lambda = x - \theta$	$(1 - B')B'' + 4B = 0.$

2.5.	$\varphi = x^3 r^{-2} B(\lambda)$, $\lambda = \alpha\theta - \ln r$	$(1+\alpha^2)B'' + 4B' + 4B - 18B^2 = 0$
2.6.	$\varphi = x^3 r^{-2} B(\lambda)$, $\lambda = \theta$	$B'' + 4B - 18B^2 = 0.$

In Submodel 2.5, the invariant surface $\lambda = \text{const}$ is located along the Ox-axis and does not intersect the flow domain. It can be a compact discontinuity or a wall, which provides us with important physical examples of flows, but cannot be regarded as a shock wave surface. Therefore, Submodel 2.5 is not of interest for our purpose. As was shown in [5], the phase portrait of the equations of Submodels 2.4 and 2.6 contains closed integral curves, which allows us to find a periodic solution for the function $B(\lambda)$.

An analysis of integral curves of the equation for $B(\lambda)$ shows that for Submodels 2.1 and 2.3 there are no continuous periodic solutions in the entire domain. This means that either the flow domain is bounded by special walls or, which is more natural, there is a shock wave in the flow domain. Since the solution is invariant from both sides of the shock wave, the shock wave surface is given by the invariant equation $\lambda = \text{const}$ [7].

The goal of this paper is to construct solutions with shock waves on nonplanary surfaces $\lambda = \text{const}$. An example of a shock wave surface is presented in Figure 1.

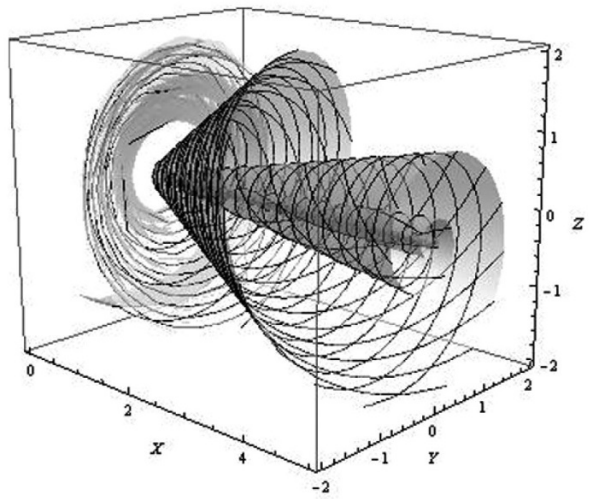

FIGURE 1. The surface $\lambda = \text{const}$ in Submodel 2.1 for $\alpha = 0, 2$ and $\beta = 1$.

3 Submodel 2.1

The solution is represented as $\varphi = x^3 r^{-2} B(\lambda)$, $\lambda = \alpha\theta + \beta \ln r - \ln|x|$, where $B(\lambda)$ satisfies the equation

$$(\alpha^2 + \beta^2 - 3B + B')B'' - 5(B')^2 + (-4\beta + 21B)B' + 4B - 18B^2 = 0. \tag{8}$$

We derive the equation for characteristic surfaces. The sound surface is given by the equation

$\varphi_x = 0$. We have

$$\varphi_x = \frac{3x^2 B(\lambda)}{r^2} - \frac{x^2 B'(\lambda)}{r^2} = 0.$$

Thus, in terms of the invariant function $B(\lambda)$ the sound surface is written as $3B = B'$.

By Equation (7), the invariant characteristic surface $h = \lambda$ can be written as

$$B' = 3B - \alpha^2 - \beta^2. \tag{9}$$

Finally, in the case $h = \lambda$, the Rankine–Hugoniot conditions (6) are written as

$$\frac{B_1' + B_2'}{2} = 3B - \alpha^2 - \beta^2, \quad [B] = 0, \quad [B'] > 0, \tag{10}$$

where the subscripts "1" and "2" denote states before and behind the shock wave. By (9), the characteristic surface separates states before and behind the shock wave.

Since Equation (8) is of the second order, it is possible to compute its admissible symmetry group which can be used for its integration. Using the standard algorithm, we arrive at the following assertion.

Proposition 1. *For arbitrary parameters α and β Equation* (8) *admits a one-parameter symmetry group with the infinitesimal operator $X = \partial_\lambda$. For $\alpha = 0$ and $\beta = 2/3$ Equation* (8) *admits an additional transformation with the operator $Y = e^{3\lambda}\partial_B$.*

The proof is too cumbersome and is omitted. In the case $\alpha = 0$ and $\beta = 2/3$, we apply the integration algorithm to find the solution

$$B(\lambda) = e^{3\lambda}\left(C_1 + \int_0^\lambda e^{-3s}u(s)ds\right), \quad 3u(\lambda)^3 - 2u(\lambda)^2 = C_2 e^{6\lambda}. \tag{11}$$

In the general case, replacing $p(B) = B'(\lambda)$, we reduce Equation (8) to the first order ordinary differential equation

$$\frac{dp}{dB} = \frac{-\big(4B - 18B^2 - 5p^2 + p(21B - 4\beta)\big)}{p(-3B + p + \alpha^2 + \beta^2)}. \tag{12}$$

3.1. Integral curves. Equation (12) has three stationary points on the plane (p, B). Two stationary points are independent of parameters:

a) $(p = 0,\ B = 0)$,

b) $(p = 0,\ B = 2/9)$,

whereas the third parameter depends on α and β:

c) $\left(B = \dfrac{5\alpha^4 + 10\alpha^2\beta^2 - 4\alpha^2\beta + 5\beta^4 - 4\beta^3}{9\alpha^2 + 9\beta^2 - 12\beta + 4}, p = \dfrac{2\left(3\alpha^4 + 6\alpha^2\beta^2 - 2\alpha^2 + 3\beta^4 - 2\beta^2\right)}{9\alpha^2 + 9\beta^2 - 12\beta + 4}\right)$.

The corresponding eigenvalues have different values and, consequently, the points can change their type:

- if $\alpha^2 + \beta^2 < 2/3$, then a is a focus (or a center if $\beta = 0$), b is a node, and c is a saddle,
- if $\alpha^2 + \beta^2 > 2/3$, then a is a focus, b is a saddle, and c is a saddle.

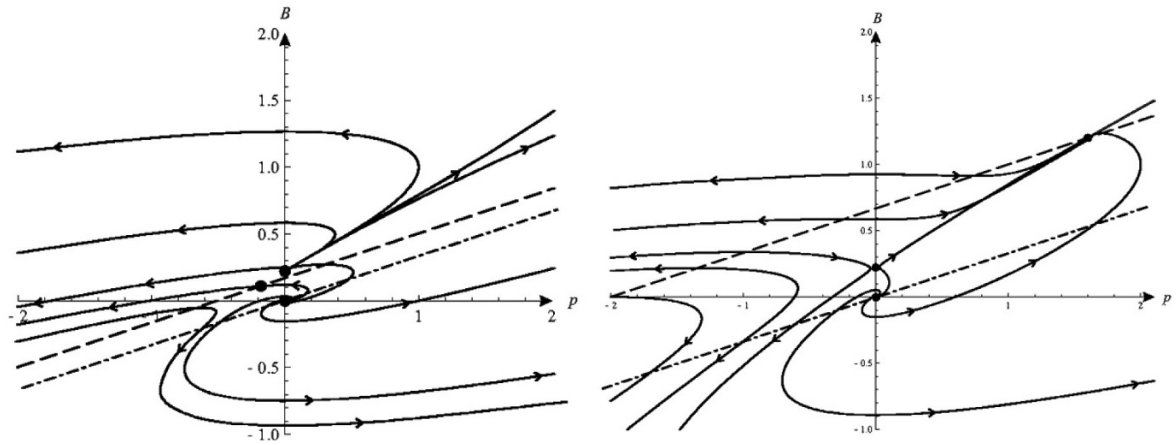

(a) (b)

FIGURE 2. The integral curves for Equation (12) in cases (a) $\alpha = 1$, $\beta = 1$ and (b) $\alpha = 0,5$, $\beta = 0,5$. Singular points are represented by bolddots, the dashed line represents transition through the characteristic surface, and the dash-and-dot line represents transition through the sound speed.

In the obtained solution (11) with $\alpha = 0$ and $\beta = 2/3$, the saddle point c tends to infinity.

Examples of phase portraits in the plane (p, B) depending on α and β are shown in Figure 2. The arrows indicate the direction of growth of λ along integral curves defined by the sign of p: the function $B(\lambda)$ decreases for $p < 0$ and increases for $p > 0$. The dash-and-dot line represents transition through the sound speed.

The fact that there are no closed trajectories on the phase plane means that there are no continuous periodic solutions to Equation (8). For the existence of a periodic solution in the entire space, one can extend the class of admissible solutions and consider solutions with shock waves.

3.2. Conditions on shock wave. The Rankine–Hugoniot conditions (10) connect the values of (p, B) before and behind jump.

Definition 1. Suppose that $p_1 = B_1'$ and $p_2 = B_2'$. Then the points $(p_1,\ B)$ and $(p_2,\ B)$ connected by Rankine–Hugoniot conditions (10) are called *conjugate*.

Conjugate points have equal ordinates and are located at the same distance from the dashed line in Figure 2, (a), (b). It is important that the shock wave does not divide the space (i.e., one can reach any side of the shock wave in a continuous way, by walking around the Ox-axis). Hence the conjugate points lie on the same integral curve.

Thus, the problem for constructing solutions with shock waves is reduced to looking for an integral curve containing two points satisfying (10), i.e., possessing the same ordinate $B(p_1) = B(p_2)$ and located at the same distance from the line:

$$B = \frac{1}{3}(p + \alpha^2 + \beta^2) \tag{13}$$

on the phase plane.

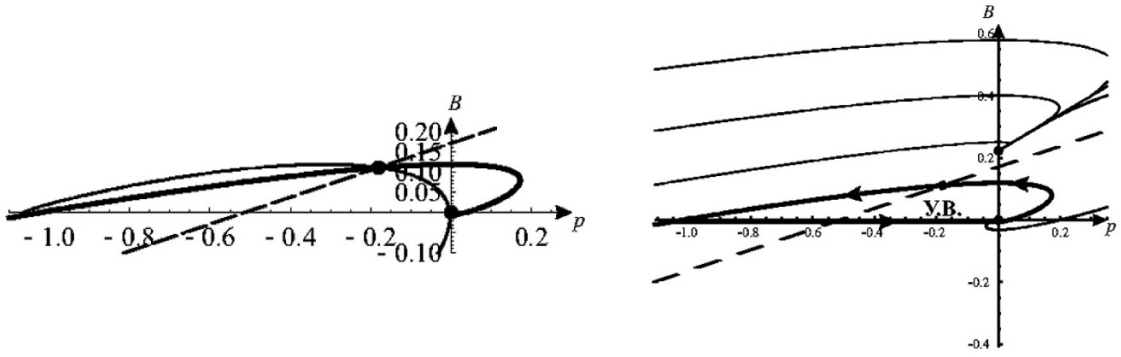

(a) (b)

FIGURE 3. Conjugate points: (a) intersection of the integral curve (the bold line) of Equation (12) and its conjugate (14) (marked by the regular line); (b) the shock wave transition corresponding (16) for the integral curve in (a) with $\alpha = 0,515966$ and $\beta = 0,5$.

3.3. Equation for conjugate points. By (10), the conjugate point has coordinates $(q(t), B(t))$, where $q = 6B - 2(\alpha^2 + \beta^2) - p$. If a point moves along the integral curve defined by Equation (12), the conjugate point defines the curve given by the equation

$$\begin{aligned} q'(t) &= B(t)(-15q(t) + 6\alpha^2 + 6\beta^2 - 24\beta + 4) + 36B(t)^2 - 2q(t) \\ &\quad \times (\alpha^2 + (\beta - 2)\beta) + q^2(t) - 8(\alpha^4 + \alpha^2\beta(2\beta - 1) + (\beta - 1)\beta^3), \\ B'(t) &= (-6B(t) + q(t) + 2(\alpha^2 + \beta^2))(-3B(t) + q(t) + \alpha^2 + \beta^2). \end{aligned} \tag{14}$$

The intersection of an integral curve and its conjugate means the existence of a pair of points satisfying Rankine–Hugoniot conditions (10) on the shock wave. Figure 3, (a) yields an example of conjugate integral curves; the bold line corresponds to the integral curve defined by (12) and the regular line corresponds to the conjugate (14).

The parameter λ should monotonically vary along the required integral curve and the curve should intersect the line (13). Therefore, we can assume that a suitable integral curve is a separatrix of a saddle singular point, which is confirmed by numerical study of Equations (12), (14). We find the values of α and β for which there are conjugate points on the separatrix.

The constructed solution satisfies the 2π-periodicity condition:

$$T = \frac{2\pi\alpha}{k}, \quad k \in \mathbb{N}, \tag{15}$$

where T is a period of the solution $B(\lambda)$.

The period of the solution $B(p)$ to Equation (12) is computed by

$$p = B'(\lambda), \quad d\lambda = \frac{B'(p)dp}{p}, \quad T = \int\limits_{p_1}^{p_2} \frac{B'(p)dp}{p}.$$

We can reach the relation (15) by the choice of α and β. A numerical experiment shows that $k = \frac{2\pi\alpha}{T} = 2,00003$ for $\alpha = 0,515966$ and $\beta = 0,5$. For

$$p_1 = 0,0085, \quad p_2 = -1,0749, \quad B_1 = B_2 = -0,0056, \quad T = 1,6209 \tag{16}$$

we have the shock wave passage as in Figure 3, (b). The arrow indicates the direction of growth of λ. For $k = 2$ there are two nested shock waves.

If a solution to Equation (12) is known, we can construct a periodic solution to Equation (8) for the function $B(\lambda)$ (cf. Figure 4). We see that the solution loses smoothness.

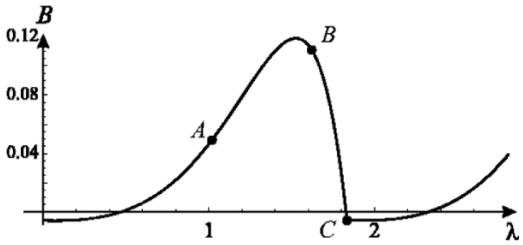

FIGURE 4. The periodic solution to Equation (8) with $\alpha = 0,515966$ and $\beta = 0,5$. The points (A), (B), and (C) represent transition through the sound speed, characteristic surface, and shock wave.

4 Submodel 2.3

In this submodel, the solution is represented as $\varphi = r^{-2}B(\lambda)$, $\lambda = x - \alpha\theta - \ln r$, where $B(\lambda)$ satisfies the equation

$$(1 + \alpha^2 - B')B'' + 4B' + 4B = 0, \tag{17}$$

and the shock wave surfaces look like in Figure 5.

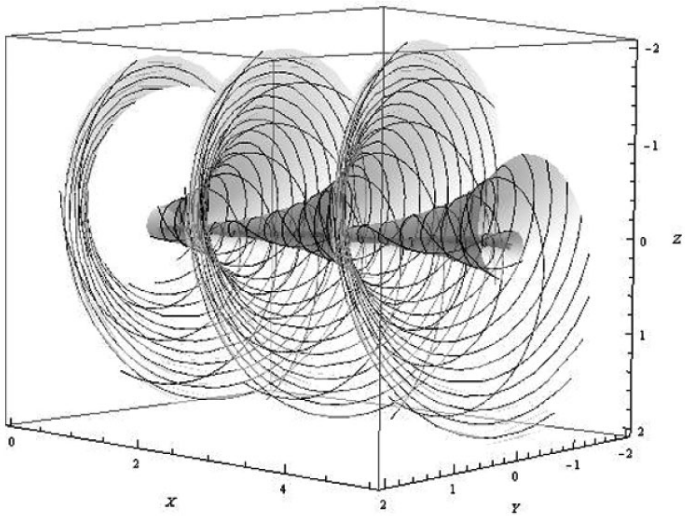

FIGURE 5. The surface $\lambda = \text{const}$ in Submodel 2.3 for $\alpha = 0,5$.

As above, setting $p(B) = B'$, we pass to the first order ordinary differential equation

$$\frac{dp}{dB} = \frac{-4(B + p(B))}{p(B)(1 - p(B) + \alpha^2)}. \tag{18}$$

On the plane (p, B), Equation (18) has two singular points $(0, 0)$ and $(1 + \alpha^2, -1 - \alpha^2)$. The first point is a focus if $\alpha \neq 0$ or a node if $\alpha = 0$, whereas the second one is a saddle. A typical picture of integral curves for $\alpha = 1$ is shown in Figure 6.

4.1. Computation of characteristic surfaces.

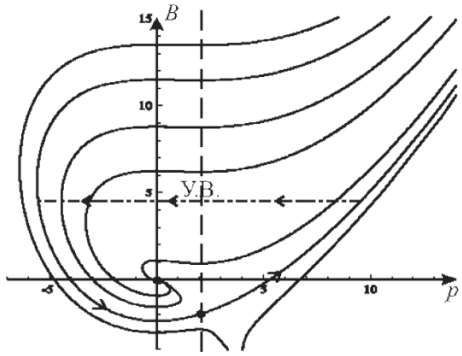

FIGURE 6. The integral curves corresponding to (19), the shock wave transition for $\alpha = 1$.

We find the equation for characteristic surfaces for submodel 2.3. We have

$$\varphi_x = \frac{B'(\lambda)}{r^2} = 0.$$

Then the sound surface is given by the equation $B' = 0$. In this case, the invariant characteristic surface described by Equation (7) has the form $B' = 1 + \alpha^2$.

The Rankine–Hugoniot conditions (6) are written as

$$\frac{p_1 + p_2}{2} = 1 + \alpha^2, \quad [B] = 0, \quad [p] < 0.$$

By the same reasons, the conjugate points lie on the same integral curve and are symmetric relative to the vertical line $B = 1 + \alpha^2$ on the phase plane. As in the case of submodel 2.1, such points are located only on the separatrix of the saddle singular point. We find the values of parameters for which conjugate points exist.

4.2. Study of the period of solutions. For solutions with shock wave in Submodel 2.3 the periodicity condition should be satisfied. The relation (15) is satisfied by the choice of α. In the case as in Figure 6, the conjugate points are as follows:

$$p_1 = -5,5484, \quad p_2 = 9,5484, \quad B_1 = B_2 = 4,513 \quad \text{with } T = 3,547. \tag{19}$$

However, in this case, for (15) $k = 1,7709$ is not integer. For $k = \frac{2\pi\alpha}{T} = 2,005$ we should have $\alpha = 1,36$. Thus, the existence of two nested shock waves is possible.

For the obtained solution to Equation (18) a periodic solution to Equation (17) for $B(\lambda)$ looks like in Figure 7.

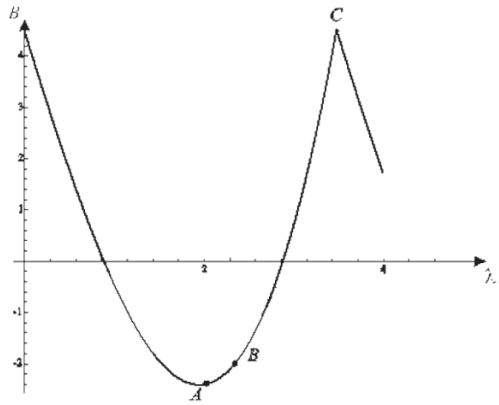

FIGURE 7. The periodic solution to Equation (17) for $\alpha = 1$. The transition through the sound speed (A), characteristics (B), and shock wave (C) are marked by the dots.

Acknowledgments

The work was supported by President Grants for Government Support of Young Russian Scientists (MD-168.2011.1) and the Leading Scientific Schools of the Russian Federation (grant No. NSh-6706.2012.1) and the Federal Target Program "Scientific and scientific-pedagogical personnel of innovative Russia" in 2009-2013 (government contract No. 02.740.11.0617).

The author thanks Professor S, V. Golovin for statement of the problem and useful remarks.

References

1. J. D. Cole and L. P. Cook, *Transonic Aerodynamics*, North-Holland, Amsterdam etc. (1986).
2. K. G. Guderley, *Theory of Transonic Flows*, Pergamon Press, Oxford etc. (1962).
3. E. G. Shifrin, *Potenrial and Vortical Transonic Flows of an Ideal Gas* [in Russian], Fizmatgiz, Moscow (2001).
4. E. O. Kuznetsova and I. A. Chernov, "Exact solutions of the transonic equations of gas dynamics" [in Russian], *Izv. Sarat. Univ., Ser. Mat.* **7**, No. 1, 54–63 (2007).
5. S. V. Golovin, "Group stratification and exact solutions of the equation of transonic gas motion" [in Russian], *Prikl. Mekh. Tekh. Fiz.* **44**, No. 3, 51–63 (2003); English transl.: *J. Appl. Mech. Tech. Phys.* **44**, No. 3, 344–354 (2003).
6. L. V. Ovsyannikov, *Lectures on the Fundamentals of Gas Dynamics* [in Russian], Nauka, Moscow (1981).
7. V. M. Men'shikov "On extension of invariant solutions to equations of gas dynamics through a shock wave" [in Russian], *Din. Splosh. Sredy* No. 4, 163–169 (1970).

Submitted on March 12, 2012